ELSEVIER

Journal of Nuclear Materials 279 (2000) 51–56

journal of nuclear materials

www.elsevier.nl/locate/jnucmat

Determination of the yield strength of nuclear reactor pressure vessel steels by means of amplitude-dependent internal friction

K. Van Ouytsel [a,b,*], A. Fabry [a], R. De Batist [c], R. Schaller [d]

[a] *SCK CEN Nuclear Research Centre, Boeretang 200, B-2400 Mol, Brussels, Belgium*
[b] *VUB Free University of Brussels, Pleinlaan 2, B-1050 Brussels, Belgium*
[c] *RUCA, University of Antwerp, Middelheimlaan 1, B-2020 Antwerp, Belgium*
[d] *Institut de Génie Atomique, Ecole Polytechnique Fédérale de Lausanne, PHB-Ecublens, CH-1015 Lausanne, Switzerland*

Received 15 July 1999; accepted 26 November 1999

Abstract

Amplitude-dependent internal friction measurements allow the determination of a critical amplitude which corresponds to the onset of plastic behaviour and is related to the yield stress (YS) in torsion. The results compare well with the YS obtained from static tensile tests on three different pressure vessel steels and can be fitted with a two- or three-component model comprising long- and short-range dislocation-defect interactions and grain-boundary effects. The effect of thermal aging is to emphasize the presence of dragging contributions to the yield strength, while neutron-irradiation results in an athermal increase in the YS related to irradiation-induced clustering.

1. Introduction

The pressure vessel is one of the major components of a nuclear reactor. It contains fuel and moderator, light water at 290°C in the present consideration, and is therefore subject to neutron irradiation and thermal aging. The regulatory guide methodology to assess the fracture toughness of light-water nuclear reactor pressure vessels (RPVs) relies on the Charpy V-notch impact test. Body centred cubic (bcc) materials exhibit a sharp transition from brittle to ductile behaviour and in the transition-temperature range, the crack-initiation and –arrest fracture toughness are taken to be universal functions, applying to all reactor pressure-vessel steels, of the nil-ductility reference temperature (RT_{NDT}). It is assumed that the influence of irradiation on the initiation and arrest fracture toughness curves can be determined simply by equating the RT_{NDT} shift to the 41 J shift (ΔTT_{41}). The main inadequacy of these regulations was found to lie in the physical basis of the unirradiated RT_{NDT} in relation to the determination of the fracture toughness [1,2].

In order to address the inadequacies of the current surveillance methodology a framework of enhanced commercial surveillance was established entailing mainly a more profound evaluation of instrumented impact test results, additional tensile testing at low temperatures, reconstitution of broken specimens and modelling aimed at working towards the development of more physically based, plant-specific surveillance programmes. Within this framework, the Belgian nuclear research centre (SCK) employs various non-destructive microstructural characterization techniques to construct the modelling pillar of enhanced surveillance in Belgium [3].

The focus, to date, is on internal friction (IF). The following discussion relates to the results which were obtained from amplitude-dependent internal friction (ADIF) measurements and provides better insight into dislocation-defect mechanisms.

Besides knowledge of the fracture toughness and the transition-temperature shift, other material properties are also determined within the frame of surveillance. In this work, the yield stress (YS), determined from in-

* Corresponding author. Tel.: +32-14 333 049; fax: +32-14 321 216.
E-mail address: kvouytse@sckcen.be (K. Van Ouytsel).

PII: S0022-3115(99)00276-7

strumented impact and tensile tests and susceptible to a variety of embrittling processes, will be discussed. From the ADIF results the YS will be derived and placed alongside and compared with the tensile YS and in this manner provide a better understanding of the dislocation-related mechanisms underlying embrittlement due to thermal aging and neutron irradiation.

2. Experimental

The internal friction experiments of the unirradiated and thermally aged specimens were carried out by means of a torsion pendulum at the Ecole Polytechnique Fédérale de Lausanne in Switzerland, while the irradiated results were obtained by means of the new torsion pendulum set up at SCK. The torsion penduli operate at around 1.5 Hz and were designed for experiments at high strain amplitudes (10^{-4}–10^{-2}) and low-to-intermediate temperatures (80–700 K). All measurements were carried out under a preliminary vacuum of approximately 10^{-5} mbar to which helium (up to 5 mbar) was added for improved thermal conductivity.

Three materials in the unirradiated condition were investigated: JRQ (A-533 B Class 1, International Atomic Energy Agency (IAEA) reference plate [4], Siemens (22Ni–Mo–Cr37 forging) [5] and (Heavy Section Steel Irradiation (HSSI) program, weld 73 W) [6,7] and will hereafter be referred to as JRQ, Siemens and HSSI respectively. Table 1 summarizes the heat treatment and states the prevailing steel microstructure. Table 2 gives the chemical composition.

The thermal aging treatment was carried out for three years in a furnace at 300°C, while the irradiated specimen was subsequently subjected to a short irradiation treatment of three weeks at 290°C to a fluence of $5 \times 10^{+19}$ n/cm^2 in the high-flux BR2 materials testing reactor. Based on the suggestion that the flux effect influences only the rate of irradiation-induced clustering, this treatment is comparable to irradiation under pressurized water reactor (PWR) conditions.

All internal friction specimens were sawn from broken impact-test specimens into $1.3 \times 1.3 \times 22/26$ mm^3 square-cross-sectional bars. Per material, only one sample was required and careful experiments have shown that well-chosen annealing treatments can be applied to bring the specimen back into its original state after each measurement, though it was not deemed necessary in every case when measurements were not carried out at strain amplitudes far exceeding the critical value.

The torsion penduli operate in free vibration and from the free decay signal, the resonance frequency of the system, F, and the internal friction, Q^{-1}, proportional to the ratio of the energy dissipated in the specimen in one cycle to the maximum elastic energy stored in the specimen, were determined.

In this study, the internal friction and the resonance frequency were investigated as a function of strain amplitude at a frequency of approximately 1.5 Hz, leading to a maximum strain rate of the order of 10^{-3}/s. The results were compared with static tensile results carried out at a strain rate of 7×10^{-5}/s.

Table 1
Heat treament and microstructure

Type of steel	ASM classification and microstructural taxonomy
JRQ	IAEA standard material, A533 B class 1 plate 225 mm thick, normalised, quenched, tempered and stress relieved, acicular ferrite/pearlite with fine tempered carbides
Siemens 22NiCrMo37A-10	DIN 22NiMoCr37 300 mm thick forging, normalised, quenched and tempered, tempered bainite
HSSI 73 W	A 533 grade B class 2 plate, 218 mm thick, submerged arc weld, stress relieved, bainite with ferrite islands

Table 2
Chemical composition

Chemical composition (wt%)	Al	C	Cr	Cu	Mn	Mo
JRQ	0.021	0.18	0.14	0.14	1.42	0.51
22NiMoCr37-A10	n.a.	0.22	0.39	0.08	0.88	0.51
HSSI 73 W	n.a.	0.098	0.25	0.31	1.56	0.58
	N	Ni	P	S	Si	Fe
JRQ	0.002	0.84	0.017	0.004	0.24	Bal.
22NiMoCr37-A10	n.a.	0.84	0.006	0.004	0.23	Bal.
HSSI 73 W	n.a.	0.60	0.005	0.005	0.45	Bal.

3. Results and discussion

3.1. Procedure

From the ADIF results, a critical amplitude corresponding to the onset of plasticity was determined. Fig. 1 describes the procedure.

Two methods to determine the internal friction, Q^{-1} and Q_{bis}^{-1} are enlightened. Q^{-1} is determined from the Fourier transform of the total free decay with exception of the first three periods and effective amplitude (effamp) represents the corresponding maximum amplitude. Q_{bis}^{-1}, on the other hand, is determined from the logarithmic decrement taken from precisely the first three periods of the free decay [8]. ε_c is taken to be the amplitude at which Q^{-1} and Q_{bis}^{-1} separate and effamp levels off. The separation between Q^{-1} and Q_{bis}^{-1} is an indication of a pronounced transition in the amplitude dependence where the method of determination of the internal friction becomes important.

The saturation of effamp is a further indication of amplitude dependence. For sufficiently large strain amplitudes, the signal will rapidly dampen and effamp will level off to an amplitude-independent value. The beginning of saturation is determined from the intersection of two linear regression lines differing markedly in slope in the transition region. In the same manner, ε_c coincides with the transition in and separation between Q^{-1} and Q_{bis}^{-1} (Fig. 1).

Both demarcations are required to give a reliable value of the critical amplitude within an error margin of $\pm 3 \times 10^{-4}$. This is attributed to pre-plastic effects in this high-amplitude region, such as partial and/or non-permanent depinning which is occasionally observed as a maximum in the ADIF. The procedure remains empirical, but since the critical amplitude is taken to represent clear and permanent break-away of dislocations from strong pinners and has been applied successfully to a wide variety of pressure vessel steels, we are confident that it is valid in the present consideration of presenting a non-destructive means to determine the onset of plastic behaviour.

The ADIF experiments are carried out at different temperatures, usually at 100, 150, 200, 250 and 300 K, and the critical stress (the YS) corresponding to the critical strain amplitude is subsequently plotted as a function of temperature.

For the purpose of comparing the internal-friction and tensile test results, the YS, σ_y, was inferred from the critical amplitude by applying the following simple equation:

$$\sigma_y(T) = \sqrt{3} G(T) \varepsilon_c(T), \tag{1}$$

where G represents the shear modulus of the material equalling 79 GPa [9,20] at room temperature and subsequently determined from the resonance frequency at the temperature investigated.

The equation is a simple approximation based on Hooke's law and accounts for the difference between yielding in tension and in torsion by applying the Von Mises criterion [9] in which only the shear stress in the horizontal plane in the reference frame of the torsion pendulum acts on the specimen.

The relation between the shear modulus and the resonance frequency f is given by

$$f = \frac{1}{2\pi} \sqrt{\frac{\beta c^4 G}{LI}}, \tag{2}$$

where $\beta = 0.141$ for square-cross-section shaped specimens, c is the thickness, L the length of the specimen, and I represents the moment of inertia used in the torsional experiments equalling 0.02 kg m^2.

Fig. 2 contains the YS data obtained from ADIF and from tensile tests carried out within the frame of an international round-robin laboratory test campaign for the IAEA reference material JRQ (data from the SCK Belgium, GKSS Germany, CEA France, JAERI Japan and AEA Technology, United Kingdom).

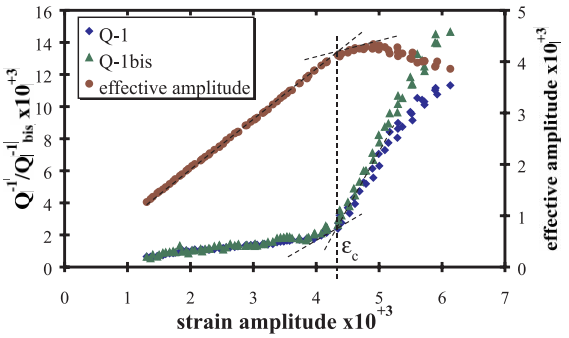

Fig. 1. Q^{-1} (curve 1), Q_{bis}^{-1} (curve 2) and effamp (curve 3) for JRQ steel in the unirradiated condition at 300 K. ε_c is the critical amplitude corresponding to the onset of plasticity.

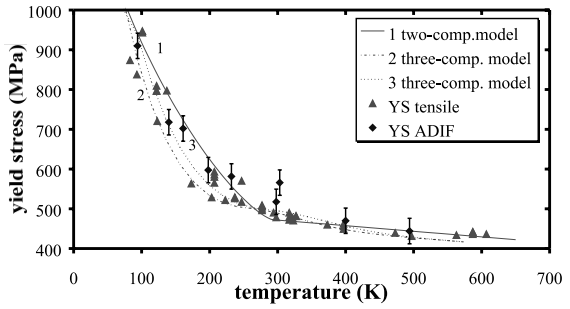

Fig. 2. Unirradiated JRQ steel. Comparison of the YS derived from ADIF with the yield stress obtained from static tensile tests and with the two- and three-component model for the YS.

The figure clearly shows the low-temperature hardening attributed to the strong temperature dependence of the mobility of screw dislocations in bcc materials [10] and emphasizes the accurate correspondence between the internal friction derived YS and the tensile test results. This illustrates the aptitude of the non-destructive internal friction technique for commercial surveillance of reactor pressure vessels. Especially for older plants, for which surveillance material is scarce, ADIF presents an advantage in that only one specimen is required to trace out the yield strength compared to a separate specimen for each point in tensile tests.

3.2. The model

The solid line in Fig. 2 represents the modelled YS $\sigma_y(T,\dot{\varepsilon})$ as a function of temperature. This model is based on two main contributions to the YS: short-range, intrinsic lattice type, and long-range dislocation–defect interactions [11–13]. The model is discussed as follows.

For temperatures above or equal to the critical temperature T_c, in the region where the intrinsic lattice (Peierls) component becomes negligible:

$$\sigma_y(T) = \sigma_0(1-\alpha T), \tag{3}$$

while for temperatures below T_c:

$$\sigma_y(T,\dot{\varepsilon}) = \sigma_0(1-\alpha T) + \sigma_p\left[1-\left(\frac{T}{T_c}\right)^{1/m}\right]^m, \tag{4}$$

where

$$T_c = \frac{H_p}{k\ln\left(\dot{\varepsilon}_0/\dot{\varepsilon}\right)}, \tag{5}$$

where σ_0 represents the athermal component of the YS, $\alpha = 2.8\times10^{-4}$ K^{-1} for iron and steel and describes the temperature dependence of the elastic modulus, σ_p is the Peierls-type component of the YS, T_c the critical temperature, dependent on the strain rate, above which the Peierls component vanishes, $m = 2$ describes the shape of the Peierls barriers, H_p the activation enthalpy for thermal activation over the Peierls hills, $\dot{\varepsilon}$ the strain rate and $\dot{\varepsilon}_0$ is the intrinsic strain rate sensitivity which measures the rate of attempts to jump the barrier, times the strain produced by a successful attempt.

The term on the right-hand side of Eq. (3) represents long-range dislocation–defect interactions involving interstitial and substitutional defect interactions, copper precipitation, carbide precipitation and grain-boundary effects. These various contributions to the YS have frequently been discussed by numerous authors, a summary of which is given in [9,12,13].

The second term of Eq. (4) describes Peierls-type short-range interactions simplified to a single rate-controlling mechanism. This second term is based on the Fleischer model [14] which includes the effect of impurities, localized strain centres, on the barriers to dislocation movement in steels.

The dotted lines in Fig. 2 represent a refinement of the two-component model. In this model, a third component σ_d is included to account for interstitial dragging effects. This involves the addition of a Gaussian contribution to Eq. (4). The model is shown for the two different strain rates: 7×10^{-5}/s for tensile results and 10^{-3}/s for ADIF results.

$$\sigma_d = \frac{a}{s\sqrt{2\pi}}\exp\left(-\frac{1}{2}\left(\frac{(T-T_{max})}{s}\right)^2\right). \tag{6}$$

The amplitude a of the dragging component is, however, small, around 40 MPa and not always observable in the YS. T_{max} represents the temperature at which the dragging component attains a maximum (approximately 333 K for JRQ) and s represents the standard deviation of the Gaussian curve. The third component was found to have an activation energy equal to that of the Peierls component, about 0.6 eV, and was thus seen as a perturbation of the dislocation–intrinsic lattice interaction which may be represented by a Gaussian function.

Even though the difference between the two models is small, the three-component model was found to fit the tensile data better. With regard to the internal friction results, the three-component model also represents a better fit of the data. The effect of strain rate is shown for the three-component model and proves to be small and lie within uncertainty limits.

3.3. Application to the Siemens and HSSI materials

Fig. 3 shows a similar correspondence between tensile and internal-friction results for a Siemens (22Ni–Mo–Cr37) steel. The two- and three-component model for the tensile strain rate and the three-component model

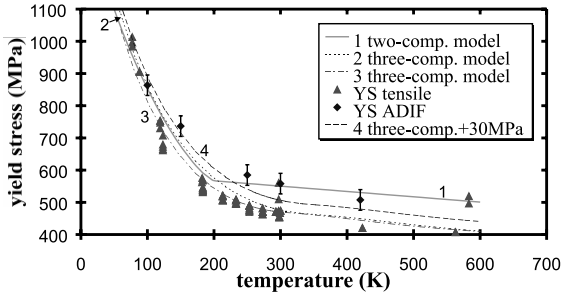

Fig. 3. Unirradiated Siemens pressure-vessel steel. Comparison of the YS derived from ADIF tests with the yield stress obtained from tensile tests (Belgium, Germany) and with the two-component model (1) (strain rate: 7×10^{-5}/s), the three-component model for the yield stress (strain rate: 10^{-3}/s (2) and 7×10^{-5}/s (3)) and the three-component model (2) +30 MPa (4).

for the torsional strain rate are displayed. Again, the three-component model is favoured over the two-component model. At around 150 and 250 K, the internal friction results are higher than predicted by the model. The lack of tensile data at around 150 K and the competition between the two- and three-component models from 250 to 600 K in both the IF and tensile data, observed also for the JRQ material, strongly suggest that the model may be enhanced with still another dragging mechanism. This is discussed in the following paragraph.

According to Schöck and Seeger [15], short-range interactions also contribute to the athermal YS. They state that the Snoek effect involving the redistribution of interstitials in a dislocation stress field resulting in the locking of the dislocations occurs fast enough for the contribution to be essentially temperature-independent.

The Snoek effect σ_s was proposed to add to the YS in the following athermal way:

$$\sigma_s = 10.25\frac{A}{b}c_i, \tag{7}$$

where A represents the interaction constant derived from the interaction energy between an interstitial and a dislocation line; $b = \sqrt{3/2}^{*} a$ the Burgers vector of a dislocation lying in the $\langle 1\,1\,1\rangle$ direction with a the lattice parameter and c_i the total concentration of interstitials.

For the JRQ and Siemens materials, Figs. 2 and 3, respectively, this contribution amounts to an increase of about 30 MPa. This remains in agreement with the tensile data and provides a better fit of the internal friction data in the 225–600 K region.

Fig. 4 portrays IF and tensile test results for the HSSI pressure-vessel steel and the two-component model for both tensile and torsional strain rates. On the basis of a large number of tensile and impact test results the two-component model was preferred for this steel.

Again the comparison is good, though on the basis of a large number of tensile and impact test results, the two-component model is preferred for this steel. The addition of the Snoek effect, +15 MPa, also improves the model-experimental data relationship.

The discrepancy between the ADIF results and the model around 150 K remains elusive, even after incorporation of the Snoek effect. In this region, however, Schöck and Seeger reported that Cottrell atmosphere locking had been considered [15] to play a role. This will be elaborated on in the discussion of the thermally aged JRQ results in the following section.

3.4. The effect of thermal aging and irradiation on the JRQ material

The effect of thermal aging for three years at 300°C and neutron irradiation at 290°C to a fluence of $5 \times 10^{+19}$ n/cm^2 for the JRQ material is depicted in Fig. 5. Thermal aging induces hardening at around 130 K. As for the HSSI material, addition of the Snoek effect does not provide the sole explanation.

On the basis of the work reported in [15], we attribute this discrepancy to the Snoek–Köster effect. From studies on Fe–C alloys indicating Cottrell cloud formation in the 500–600 K temperature region [16], we propose that thermal aging of the JRQ material allows the formation of Cottrell atmospheres in the neighbourhood of the dislocation. At the low-temperatures in the thermally activated region of the YS, these atmospheres lock the dislocations resulting in an increase in the YS. Confirmation of the existence of the Snoek–Köster effect in the thermally aged JRQ steel is found in the appearance of the Snoek–Köster peak at around 540 K in the temperature-dependent internal friction results published in [17].

Neutron irradiation results in an athermal increase in the YS which is attributed to the interaction between dislocations and irradiation-induced copper-rich pre-

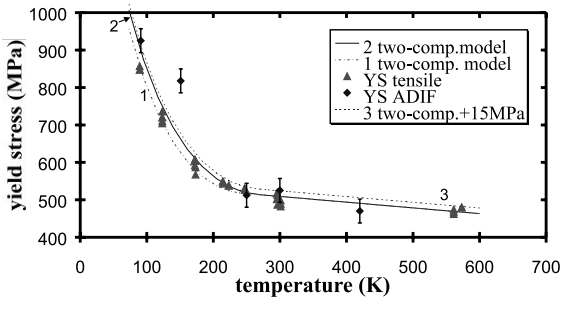

Fig. 4. Unirradiated HSSI weld material. Comparison of the YS derived from ADIF tests with the yield stress obtained from tensile tests (Belgium, US) and with the two-component model (strain rate: 10^{-3}/s (2) and 7×10^{-5}/s (3)) for the YS.

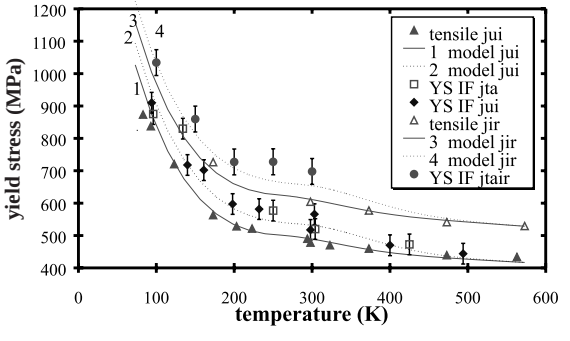

Fig. 5. The effects of thermal aging and neutron irradiation on the JRQ pressure-vessel steel. Comparison of the YS derived from ADIF with the yield stress obtained from tensile tests and with the three-component model for the YS.

cipitates containing also manganese, nickel and iron [18]. Neutron-irradiation furthermore removes interstitial atoms from solution [19,21,22]. As observed by Wechsler [19], irradiation under pressurized water reactor conditions induced nitrogen-stabilized dislocation loops, preventing the formation of glissile loops and thus aiding hardening while at the same time strongly inhibiting the formation of Cottrell atmospheres, thus eliminating the Snoek–Köster effect observed after thermal aging.

4. Conclusion

A procedure to determine the YS of three different pressure-vessel steels from ADIF results has been presented. The results compare very well with tensile data and can be fitted with a two- or three-component model comprising long- and short-range dislocation–defect interactions and a third component attributed to dislocation dragging of interstitial atoms. The internal-friction technique offers the advantage that only one specimen is required to trace out the YS as a function of temperature. ADIF furthermore reveals that the model can be improved through addition of the Snoek effect.

Thermal aging reveals the influence of Snoek–Köster-type dragging of interstitials which offers an explanation for the discrepancies observed in the 130–150 K temperature range. Neutron irradiation results in the athermal increase of the YS attributed to copper-rich precipitation and the elimination of interstitials from solid solution.

The next step in this study will be to investigate more in depth the discrepancies and their origin and apply the model to a wider range of pressure vessel steels.

References

[1] A. Fabry, E. van Walle, R. Chaouadi, J.P. Wannijn, A. Verstrepen, J.L. Puzzolante, T. Van Ransbeeck, J. Van de Velde, T. Petrova, RPV steel embrittlement: damage modeling and micromechanics in an engineering perspective, SCK CEN Mol, BLG-649 (1993) 2.
[2] K. Ohnishi, H. Tsukada, K. Suzuku, T. Iwadate, Y. Tanaka, Nucl. Eng. Design 128 (1991) 125.
[3] A. Fabry, J. Van de Velde, E. van Walle, R. Chaouadi, J.-L. Puzzolante, T. Van Ransbeeck, K. Van Ouytsel, L. Van Hoorebeke, P. de Bakker, R. Gérard, IAEA Specialists meeting on 'Technology for Lifetime Management of Nuclear Power Plants' Tokyo, Japan, 15–17 November 1994, p. 1.
[4] E. van Walle, Euratom Research Framework Programme 1994–1998: Nuclear Fission Safety AGE-RESQUE 1998, p. 125.
[5] F. Mudry, M. Di Fant, IRSID report, No. RE 93.319, 1993.
[6] R.K. Nanstad, F.M. Haggag, D.E. McCabe, S.K. Iskander, K.O. Bowman, B.H. Menke, Irradiation effects on fracture toughness of two high-copper submerged-arc welds, HSSI series 5, NUREG/CR-5913, 1992.
[7] R. Chaouadi, E. van Walle, A. Fabry, M. Scibetta, J. Van de Velde, Fracture toughness of precracked Charpy specimens of irradiated 73W weld material, in: M.L. Hamilton, A.S. Kumar, S.T. Rosinski, M.L. Grossbeck (Eds.), Proceedings of the 19th International Symposium on Effects of Radiation on Materials, ASTM STP 1366, 1999.
[8] A. Munier, PhD thesis, Ecole Polytechnique Fédérale de Lausanne, 1991, pp. 51–57.
[9] G.E. Dieter, Mech. Metall., McGraw-Hill, New York, 1986, p. 202.
[10] A. Seeger, C. Wüthrich, Nuovo Cim. 33B (1) (1976) 38.
[11] A. Fabry, R. Chaouadi, J.L. Puzzolante, J. Van de Velde, E.C. Biemiller, S.T. Rosinski, R.G. Carter, in: R.K. Nanstad, M.L. Hamilton, F.A. Garner, A.S. Kumar (Eds.), Proceedings of the 18th International Symposium on Effects of Radiation on Materials, ASTM STP 1325, 1997, pp. 452–458.
[12] K. Mazanec, E. Mazancová, Physical Metallurgy of Hermomechanical Treatment of Structural Steels, Cambridge University, Cambridge, 1997, p. 5.
[13] M.E. Natishan, David Taylor Research Centre, Bethesda, 1989, p. 5.
[14] R.L. Fleischer, Acta Metall. 10 (1962) 835.
[15] G. Schöck, A. Seeger, Acta Metall. 7 (1959) 469.
[16] L.B. Magalas, J. Phys. (Paris) IV C8 suppl. au Journal de Physique III 6 (1996) C8–163–172.
[17] K. Van Ouytsel, R. De Batist, R. Schaller, Dislocation–defect interactions in nuclear reactor pressure-vessel steels investigated by means of internal friction, ICIFUAS-12, Buenos Aires, Argentina, 9–13 July 1999, Journal Alloys and Compounds, to be published.
[18] M.K. Miller, M.G. Burke, J. Nucl. Mater. 195 (1992) 68.
[19] M.S. Wechsler, Trans. ASME 101 (1979) 114.
[20] H. Willems, H. Persch, Nuclear Science and Technology, Reactor Safety Programme 1985–1987, EUR 12621 EN (1990) 36.
[21] K. Linga Murty, Mater. Sci. Forum 97–99 (1992) 519.
[22] K. Linga Murty, Scripta Metall. 18 (1984) 87.